Design of Supercritical Cascades with High Solidity

José M. Sanz*
Universities Space Research Association, Columbia, Maryland

The method of complex characteristics of Garabedian and Korn has been used successfully to design shockless cascades with solidities of up to one. A new code has been developed using this method and a new hodograph transformation of the flow onto an ellipse. This new code allows the design of cascades with solidities of up to two and larger turning angles. The equations of potential flow are solved in a complex hodograph-like domain by setting a characteristic initial-value problem and integrating along suitable paths. The topology that the new mapping introduces permits a simpler construction of these paths of integration.

I. Introduction

THE design of supercritical blades for turbomachinery relies heavily on the capability of producing a wide variety of two-dimensional blade sections, spanning from hub to tip and varying from upstream to downstream stages. A code to design these sections will have to cover a broad spectrum of design flow conditions. It should be able to handle both low and high solidities, chord-to-gap ratios of up to two, as well as high-incidence angles and Mach numbers.

The method of complex characteristics and hodograph transformation developed by Bauer et al.[1] to design supercritical wing sections and cascades has been used widely. With this method, excellent shockless airfoils have been designed and tested in this country and abroad. In its latest version, the method solves the problem of finding a shockless airfoil with a given pressure distribution.

Because of the conformal mapping used by Bauer et al. to transform the hodograph domain of the flow onto a circle, a restriction exists in their method which does not allow the design of cascades with high solidities. Also, a poor resolution at the leading- and trailing-edge regions may arise, in cases of high-incidence angles, as a consequence of this mapping.

In this paper a new design technique is described, based on the same complex characteristics method, which uses a new mapping of the hodograph domain onto an ellipse. This new mapping leads naturally to the use of Tchebicheff polynomials, rather than trigonometric polynomials, to construct the solution of the equations. The equations of flow are integrated along a new set of paths which are more in accord with the topology that the elliptic mapping introduces.

The heuristic idea behind the elliptic mapping is the following. When the flow is mapped onto a circle, the upstream and downstream points of infinity are mapped into two interior points of the circle, where two logarithmic singularities of the solution, a source and a sink, are located. By increasing the separation between these two points, the gap-to-chord ratio can be reduced. The limiting case of infinite gap-to-chord ratio, or the isolated airfoil, corresponds to the case in which both singularities coalesce. By mapping the flow onto an ellipse, the two singularities can be more widely separated, further reducing the gap-to-chord ratio. A parameter related to the eccentricity of the ellipse will be introduced to control the solidity of the cascade.

Presented as Paper 82-0954 at the AIAA/ASME Third Joint Thermophysics, Fluids, Plasma and Heat Transfer Conference, St. Louis, Mo., June 7-11, 1982; submitted June 18, 1982; revision received Jan. 3, 1983.

*Visiting Research Scientist; presently at NASA Lewis Research Center, Fluid Mechanics and Acoustics Division, Computational Fluid Mechanics Branch, Cleveland, Ohio. Member AIAA.

With this new method we have achieved high solidities. A good resolution of points defining the body is obtained both at the leading- and trailing-edge regions and larger incidence angles, with thinner airfoils, can be achieved. In the next section we review the method of complex characteristics, as applied to our problem.

II. Hodograph Complex Equations

The equations of potential flow in hodograph coordinates can be described by the Chaplygin system,

$$\varphi_q = \frac{M^2-1}{\rho q}\psi_\theta \qquad \varphi_\theta = \frac{q}{\rho}\psi_q \tag{1}$$

in which φ and ψ are the potential and stream functions; M is the local Mach number; q and θ, respectively, the modulus and argument of the velocity vector; and ρ is the density. This system of equations is of mixed type, elliptic and hyperbolic, in the transonic regime.

In the method of complex characteristics, the variables are extended analytically into the four-dimensional domain of two complex variables, where the characteristic equations can always be solved. System (1) can be written in the canonical form,[1]

$$\varphi_\xi = \tau_+ \psi_\xi, \quad \varphi_\eta = \tau_- \psi_\eta; \quad \tau_\pm = \pm i\frac{\sqrt{1-M^2}}{\rho} \tag{2}$$

The two independent variables ξ and η are arbitrary complex analytic functions of the characteristic coordinates

$$s = \log h - i\theta, \qquad t = \log h + i\theta \tag{3}$$

where h is defined by

$$h(q) = h(C_*)\exp\left(\int_{C_*}^{q} \sqrt{1-M^2}/q'\,\mathrm{d}q'\right)$$

$$h(C_*) = \exp\left(\int_{1}^{C_*} \sqrt{1-M^2}/q'\,\mathrm{d}q'\right) \tag{4}$$

and C_* is the critical speed.

We recall that the coordinates s and t are conjugated characteristics coordinates[1] in the subsonic domain. This means that, for subsonic points, s and t are complex conjugate numbers when q and θ are real. If the variables ξ and η are defined in the form

$$s = f(\xi), \qquad t = \overline{f(\bar{\eta})} \tag{5}$$

with f analytic; then, they are also conjugate coordinates. Under this transformation the sonic surface is mapped onto a curve of each characteristic plane, called the sonic locus.[1]

In the hodograph method, we are interested in solving an inverse problem. We construct a solution with the correct logarithmic singularities, which represent a sink and source at infinity, and we look at the zero streamline, on the physical real plane, as the possible candidate for the body which generates the flow.

In the context of the complex system (2), the correct mathematical problem to solve is the characteristic initial-value problem where initial data is given in the two characteristic planes emanating from the initial point (ξ_0,η_0) in the four-dimensional space. The manipulation of the initial data can lead to the construction of shockless solutions, and it has previously.[1] A new and fundamental approach in the application of hodograph methods was taken in Ref. 2, where the unknown domain of the flow is mapped onto the unit circle, by a conformal mapping of the type Eq. (5). This allows for a systematic prescription of the initial characteristic data, based on a given pressure distribution over the airfoil. In the next section we describe how this idea is implemented.

III. Elliptic Conformal Transformation

Following the idea described in the last paragraph, we use the transformation Eq. (5) to map the flow onto an elliptic domain D of each coordinate characteristic plane. Because of this transformation, the coordinate characteristics are such that real subsonic points correspond to the domain of points of the form $(\xi,\bar{\xi})$, when ξ is a point enclosed by the portion of the boundary of D where ξ and η are conjugate coordinates and the sonic locus. This part of the boundary will correspond to the subsonic part of the body. Points in the remainder of the domain D do not correspond to the real physical plane, and the real supersonic part of the body has to be found by searching for the zero streamline.

The elliptic domain and the corresponding Tchebycheff polynomials can be defined in the following form. Consider the conformal mapping

$$\omega = \tfrac{1}{2}[\xi + (1/\xi)], \qquad 1 \le |\xi| \le R \tag{6}$$

of a circular ring in the plane onto the ellipse with axes defined by the points

$$\pm\tfrac{1}{2}[R + (1/R)], \qquad \pm\tfrac{1}{2}[R - (1/R)]$$

and the slit $(-1,1)$. We consider the class of analytic functions in the ring which have a Laurent expansion of the form

$$F(\xi) = \sum_{-\infty}^{\infty} a_n \xi^n = \sum_{0}^{\infty} a_n \left(\xi^n + \frac{1}{\xi^n}\right) \tag{7}$$

in which $a_n = a_{-n}$ for all positive n. The functions of the variable ω

$$T_n(\omega) = \frac{1}{2^n}\left(\xi^n + \frac{1}{\xi^n}\right), \qquad n = 0,1,2,\ldots \tag{8}$$

are actually the Tchebycheff polynomials of the first kind, as can be verified easily.

We observe that a function of the type Eq. (7) has the property

$$F(e^{i\theta}) = F(e^{-i\theta}), \qquad 0 \le \theta \le \pi \tag{9}$$

This means that within this class of functions, we are identifying points with the same real part in the positive and negative parts of the unit circumference. Any analytic function on the ellipse in the ω plane can then be written in the form

$$F(\omega) = \sum_{0}^{\infty} a_n \left(\xi^n + \frac{1}{\xi^n}\right) = \sum_{0}^{\infty} a_n' T_n(\omega) = \sum_{0}^{\infty} b_n \omega^n \tag{10}$$

This shows that the ellipse is equivalent to the circular ring with the given identification of points on the unit circumference. This identification actually makes unnecessary the slit introduced by the mapping equation (6), making the elliptic domain singly connected.

We adopt as our computational domain D the circular ring $1 \le |\xi| \le R$, with the previous identification of points. The parameter R will control the eccentricity of the ellipse and, in this way, the solidity of the cascade. Several advantages arise from this formulation. The most important one is that we are now able to use fast Fourier transform (FFT) to compute the coefficients of the mapping function

$$f(\xi) = \sum_{0}^{\infty} a_n \left(\xi^n + \frac{1}{\xi^n}\right) \tag{11}$$

of the flow onto our computational domain D. Other advantages of this formulation will be discussed later.

The supercritical design problem can be formulated as follows. Find an analytic solution

$$\begin{aligned}\varphi(\xi,\eta) &= R_e\{\varphi_1(\xi,\eta)\log(\eta-\eta_1) \\ &\quad + \varphi_2(\xi,\eta)\log(\eta-\eta_2) + \varphi_3(\xi,\eta)\} \\ \psi(\xi,\eta) &= R_e\{\psi_1(\xi,\eta)\log(\eta-\eta_1) \\ &\quad + \psi_2(\xi,\eta)\log(\eta-\eta_2) + \psi_3(\xi,\eta)\}\end{aligned} \tag{12}$$

of the system Eq. (2), with $\varphi_1,\varphi_2,\varphi_3$ and ψ_1,ψ_2,ψ_3 regular functions, in the domain D, where the mapping function f defined by Eq. (11), satisfies the Dirichlet condition

$$R_e\{f(\xi)\} = \log(h^*(q)), \qquad |\xi| = R \tag{13}$$

and the stream function satisfies the boundary condition

$$R_e\{\psi(\xi,\bar{\xi})\} = 0, \qquad |\xi| = R \tag{14}$$

The stream function is real valued for subsonic points and the boundary condition Eq. (4) is well defined when a proper branch of the solution is taken. The function h^* is defined by

$$h^*(q) = h(C_*)\exp\left(k\left|\int_{C_*}^{q} \sqrt{1-M^2}\,dq'/q'\right|\right) \qquad k>0 \tag{15}$$

The regular part of the solution can be expanded as a linear combination of particular solutions obtained by taking as initial characteristic data a complete set of orthonormal functions, namely, the Tchebycheff polynomials. The coefficients of this linear combination are then determined by imposing the boundary condition Eq. (14). This boundary-value problem has been proved to be well posed when the system Eq. (1) is reduced to Tricomi equation,[4] that is, in the case of the transonic small disturbance equation. In the general case of the full potential equation that we are dealing with here, a low condition number for the matrix associated with the linear system in question, both when the domain D is a circle or an ellipse, indicates the well posedness of the problem.

With the definitions given, h^* and h become identical in the subsonic part of the domain D, where we take the parameter k equal to unity. In the remainder of this domain, h is not real and the introduction of the function h^* becomes necessary. The consequence of using this Dirichlet condition is that the designed airfoil will not achieve the prescribed pressure distribution on the supersonic part of the airfoil.

The boundary conditions (13) and (14) are nonlinearly coupled. The nonlinearity of the problem arises from the fact that the speed distribution is given as a function of the arc length, and in Eq. (13) it is needed as a function of the coordinate ξ on the boundary $|\xi| = R$. The relationship between ξ and the arc length s can only be determined when the potential function is known. On the other hand, the solution of the boundary-value problem Eq. (14) is linked to

the knowledge of the mapping function f. An iterative procedure is then needed to solve the problem.

This iterative procedure is established by first computing an incompressible solution $\varphi(\xi)$, $\psi(\xi)$ on the elliptic domain, in terms of classic Jacobi elliptic functions. The incompressible solution is conformal invariant. We can then establish the relation between the length s and the boundary variable $\xi = Re^{i\theta}$, since we know $\varphi(s)$. This allows computation of the mapping function f, using FFT to solve the Dirichlet problem Eq. (13) with prescribed values of h^* at a number N of equidistant nodes on the circumference of radius R.

Once the mapping function is known, the system Eq. (2) can be integrated, since $\tau_\pm$ are known functions of the variables ξ and η. We note that at each iteration an analytic solution is found. If the zero streamline is not self intersecting and has the proper closure at the trailing edge, it represents a shockless airfoil.

IV. Numerical Solution

We concentrate in this section on the problem of finding a solution of the type of (12) to system of (2), once the mapping function f has been determined. We introduce the notation

$$L_\xi(\varphi,\psi) = \varphi_\xi - \tau_+ \psi_\xi \qquad L_\eta(\varphi,\psi) = \varphi_\eta - \tau_- \psi_\eta$$

The requirement that the functions of Eq. (12) are solutions of the system (2) with the pairs $(\varphi_i,\psi_i)\, i=1,3$ being regular functions leads to the homogeneous system, for each value $i=1,2$ of the index i,

$$L_\xi(\varphi_i,\psi_i) = 0 \qquad L_\eta(\varphi_i,\psi_i) = 0 \tag{16}$$

with

$$\varphi_i = \tau_+ \psi_i \quad \text{on} \quad \eta = \eta_i, \quad i=1,2 \tag{17}$$

and to the inhomogeneous system

$$L_\xi(\varphi_3,\psi_3) = 0 \qquad L_\eta(\varphi_3,\psi_3) = -\left(\sum_{i=1}^{2} \frac{\varphi_i - \tau_+ \psi_i}{\eta - \eta_i} \right) \tag{18}$$

Problem (16) with condition (17) is known as the Riemann problem for that system. The solutions are the Riemann functions related to that problem and can be integrated explicitly along the characteristic $\eta = \eta_i$, in the form

$$\psi_i(\xi,\eta_i) = \frac{C_i}{\sqrt{\tau_+(\xi,\eta_i)}} \qquad \varphi_i(\xi,\eta_i) = C_i \sqrt{\tau_+(\xi,\eta_i)} \tag{19}$$

and $i=1,2$.

The complex constants C_1 and C_2 remain at our disposal. These two sets of Riemann functions can be integrated with a finite difference scheme, that will be described later. We can impose on the $\xi = \xi_i$, $i=1,2$, characteristics the initial data

$$\psi_i(\xi_i,\eta) = \overline{\psi_i(\bar\eta,\bar\xi_i)} \qquad \varphi_i(\xi_i,\eta) = \overline{\varphi_i(\bar\eta,\bar\xi_i)} \tag{20}$$

Once these functions are determined, we can integrate the inhomogeneous system (18). For that, we expand the solution in the form

$$\varphi_3 = \varphi_3^{(0)} + \sum_1^N b_n \varphi_3^{(n)} \qquad \psi_3 = \psi_3^{(0)} + \sum_1^N b_n \psi_3^{(n)} \tag{21}$$

where $(\varphi_3^{(0)}, \psi_3^{(0)})$ is a solution of the inhomogeneous problem (18) with the homogeneous initial characteristic data

$$\psi_3^{(0)}(\xi,\eta_3) = \overline{\psi_3^{(0)}(\bar\eta_3,\bar\xi)} = 0 \tag{22}$$

assigned on the two characteristics emanating from a point $(\xi_3,\bar\xi_3)$, which is subsonic and far from the singularities $(\xi_1,\bar\xi_1)$ and $(\xi_2,\bar\xi_2)$. Each pair of functions $(\varphi_3^{(n)}, \psi_3^{(n)})$ are solutions of the homogeneous system (16), with the initial characteristic data

$$\psi_3^{(n)}(\xi,\eta_3) = \overline{\psi_3^{(n)}(\bar\eta_3,\bar\xi)} = T_n(\omega), \qquad n=1,\ldots,N \tag{23}$$

and where the $T_n(\omega)$ are the Tchebycheff polynomials described in Eq. (8). Once each of these initial characteristic problems is numerically solved, the coefficients b_n on Eq. (21) can be determined by imposing the boundary condition (14).

A rectangular grid is used to solve each initial characteristic problem numerically. Two sides of this rectangular grid are formed by two paths of integration, one in each characteristic plane. These paths allow one to reach the desired part of the flow to be computed. Three kinds of paths of integration are used, subsonic, transonic, and supersonic.

To reduce the amount of computation, we divide the exterior circumference into eight sectors, and we always take as initial point $(\xi_3,\bar\xi_3)$ the identical points $(0,1)$ and $(0,-1)$. From each singularity $(\xi_1,\bar\xi_1)$ and $(\xi_2,\bar\xi_2)$ we lay a path which goes directly to the point $(\xi_3,\bar\xi_3)$ to compute the Riemann solutions. The corresponding η path will be the complex conjugate of the ξ path. Once we reach the characteristics through the point $(\xi_3,\bar\xi_3)$ we continue computing the Riemann solutions plus the solution of the inhomogeneous problem (18) in the way described.

In those sectors in which all the nodes are subsonic points, we use subsonic paths. In this case the η path is the complex conjugate of ξ path. As ξ and η are conjugate coordinates at subsonic points, the diagonal of the rectangle corresponds to real subsonic points. The initial data have been defined previously by the reflection laws (20), (22), and (23). In this form the computation can be reduced to the triangle below the diagonal. A path will consist, then, of a segment that starts at ξ_3, ends at the outer circle, and continues with the circular arc corresponding to the sector in question.

In those sectors below the sonic locus, where all or some of the nodes do not correspond to real subsonic points, we use transonic paths. The idea is that to reach those points beyond the sonic line, the two-dimensional manifold formed by the two paths has to avoid the sonic surface $M(\xi,\eta) = 1$, where the equations become ill conditioned. So, in the case of those paths, we want the ξ and η paths to not be conjugates of each other. The idea is to traverse the corresponding sector in opposite directions for each path, as in Ref. 1.

Finally, the supersonic paths compute the real supersonic zone of the body. They were introduced first by Swenson and they use the property that a point in the real supersonic zone can be reached by two characteristics starting at the sonic locus of each characteristic plane.[1,5] The computation for the supersonic zone is done once the coefficients b_n in Eq. (21) have been obtained. So the problem in Eq. (18) is solved only once for these points. This makes affordable, both in terms of computing storage and CPU time, the use of a much finer grid for the supersonic computation. The analytic solution is path independent, by the Cauchy integral theorem, provided that we stay on the proper branch of the solution.

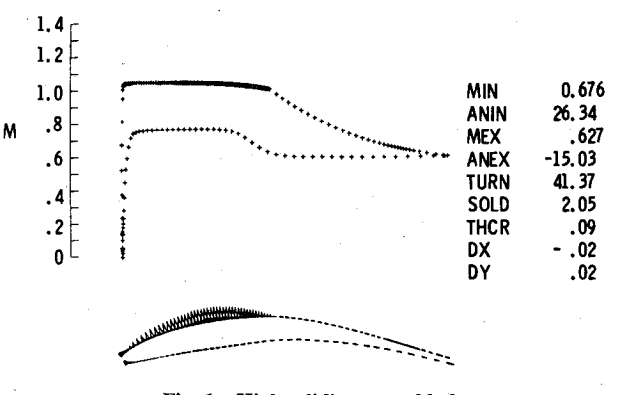

Fig. 1 High solidity stator blade.

The finite difference scheme

$$\varphi_{i,j}-\varphi_{i-1,j}=\tilde{\tau}_+(\psi_{i,j}-\psi_{i-1,j}) \quad \varphi_{i,j}-\varphi_{i,j-1}=\tilde{\tau}_-(\psi_{i,j}-\psi_{i,j-1}) \tag{24}$$

is used to integrate the equations. The average values $\tilde{\tau}_\pm$ are calculated with a predictor-corrector scheme which gives second-order accuracy. A Richardson extrapolation to the zero limit included in the code gives third-order accuracy.

Two complex constants were left at our disposal in the computation of the Riemann functions. To determine them we require, first, the stream function to be single valued along the airfoil. This leads to the condition for the jump in ψ

$$[\psi]=-2\pi[I_m\psi_1(\xi_1,\bar{\xi}_1)+I_m\psi_2(\xi_2,\bar{\xi}_2)]=0 \tag{25}$$

On the other hand, the circulation Γ over the airfoil is given. This imposes the jump condition on φ

$$I_m\{\varphi_1(\xi_1,\bar{\xi}_1)\}-I_m\{\varphi_2(\xi_2,\bar{\xi}_2)\}=\Gamma/2\pi \tag{26}$$

The location of the stagnation point and trailing edge impose the two remaining conditions needed to determine the four real constants.

With the potential function and stream function completely determined, the body is calculated using the formula

$$x+iy=\int\frac{e^{i\theta}}{q}\left(\mathrm{d}\varphi+\frac{i}{\rho}\mathrm{d}\psi\right) \tag{27}$$

By looking at the residuum of this function, when a loop is described around one singularity, say the source $\xi=\xi_2$, we obtain the repeating vector

$$[x+iy]=-2\pi\frac{e^{i\theta_2}}{q_2}\left[I_m\{\varphi_2(\xi_2,\bar{\xi}_2)\}+\frac{i}{\rho_2}I_m\{\psi_2(\xi_2,\bar{\xi}_2)\}\right] \tag{28}$$

The modulus of this vector is the gap, or distance between adjacent blades. If we consider, instead, a loop which contains both singularities, we obtain the jump in the function $x+iy$ around the airfoil

$$[x+iy]=-2\pi\left[\sum_{j=1}^{2}\frac{e^{i\theta_j}}{q_j}\left(I_m\{\varphi_j(\xi_j,\bar{\xi}_j)\}+\frac{i}{\rho_j}I_m\{\psi_j(\xi_j,\bar{\xi}_j)\}\right)\right] \tag{29}$$

The real and imaginary parts of this vector measure the opening of the airfoil at the trailing edge in the x and y directions, respectively. This formula can be used to check the accuracy of the computation, when the actual coordinates of the body are obtained.

V. Results

A computer code has been written to implement the method described. The purpose of the code is to extend the possibilities of the Bauer-Garabedian-Korn design code. We have followed, when possible, their method. A different strategy is used in the numerical solution of the equations, because of the different domain into which the flow is mapped.

The code uses as input a given speed distribution. Other parameters used include the following: the external radius R of the circular ring, which controls the solidity; the number of nodes in the exterior circle, equal to the number of Tchebycheff polynomials used in the expansion of the regular part of the solution; and the number of iterations, which controls the total number of cycles (each one includes the calculation of the mapping function and a complete solution of the equations). Additionally, two grid sizes can be set, one for the subsonic-transonic computation, and the other, a finer one, for the supersonic computation. A Richardson extrapolation can be included in the last iteration. The inlet Mach number is specified in the case of compressor design, and the exit Mach number is specified in the case of turbines.

A typical run takes 8 min of IBM 370-3033 CPU time. Note that, while a blade design can imply many runs to achieve the desired design conditions, most of these runs can be executed with a coarse grid, small number of nodes, and only one iteration, which can reduce the CPU time of each run to less than 1 min, until the approximate design conditions are obtained.

Figure 1 represents a high-solidity cascade designed with the new code. A solidity of 2.05 was obtained, with a turning angle of 42 deg. The supersonic zone reached, though, has a moderate peak Mach number of 1.07. We use 128 nodes which delivers 193 computed points on the body. It can be seen that a good resolution of points is obtained both at the leading and trailing edge. In this figure each computed body point is represented by a segment oriented in the corresponding flow direction. The stagnation point is not shown as it does not have a direction attached. This explains the apparent gap at the leading edge. Figure 2 represents the same body when a cubic spline is passed through all computed points. Figure 3 represents a typical hodograph plane with the integration paths. Figure 4 shows a highly staggered rotor tip section with an inlet flow angle of 55 deg.

Fig. 2 High solidity stator blade.

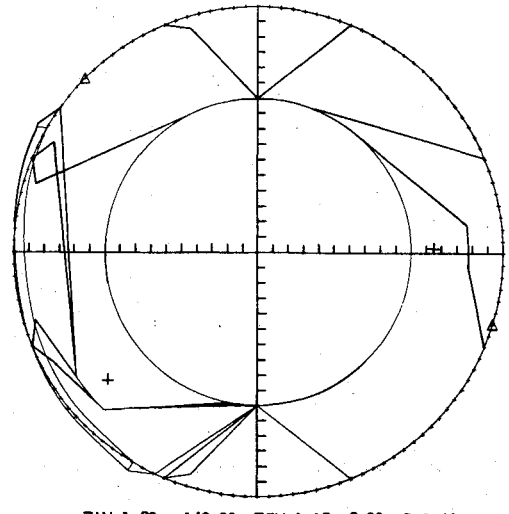

Fig. 3 Hodograph plane.

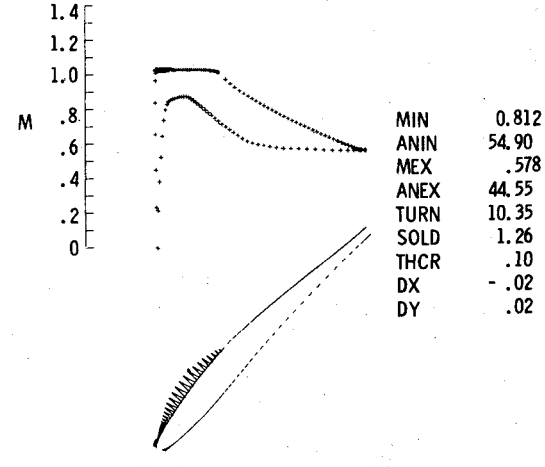

Fig. 4 High stagger rotor blade.

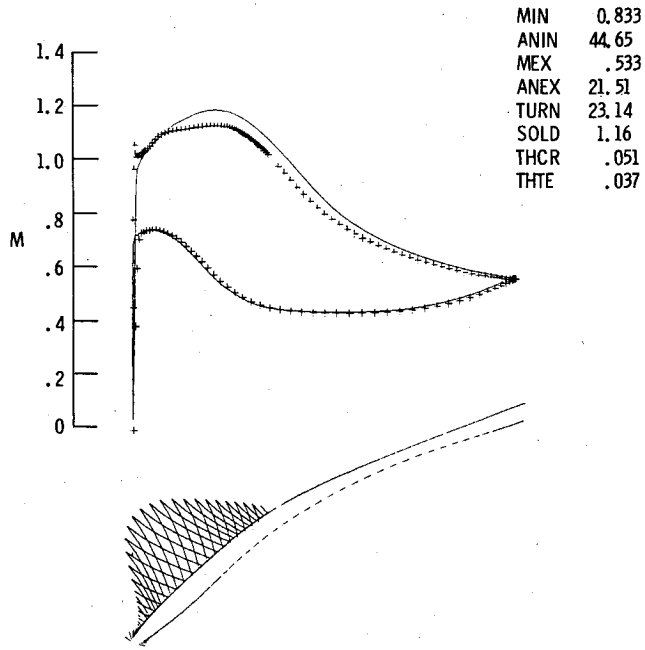

Fig. 5 Accelerated surface Mach number distribution.

The airfoils shown in Figs. 1 and 4 have a "flat top" surface Mach number distribution, a concept that has been used in the past to design good supercritical airfoils. Figure 5 shows a thin supercritical airfoil, suitable for a tip section of a compressor rotor blade, with an accelerated Mach number distribution instead of a "flat top" distribution. The surface peak Mach number of 1.14 is reached at approximately 30% of the chord and, subsequently, the flow decelerates. By delaying the appearance of an adverse pressure gradient to a 30% of the chord, the boundary-layer transition to turbulence would be expected to be delayed to this point. In this figure, the solid line represents the input Mach number distribution. The plus signs represent the design surface Mach number distribution obtained.

VI. Conclusions

A new design method has been developed for the design of supercritical cascades based on an elliptic conformal transformation of the hodograph plane and the use of complex characteristics. With this new method we have been able to handle high-solidity cascades.

Because we use, as in the Bauer-Garabedian-Korn method, an input pressure distribution the code can be coupled easily with a boundary-layer calculation. In this way, the pressure distribution can be modified until the desired separation criterion is met.

The effects of the streamtube convergence and radius change in the design of turbomachinery blades are well known. The incorporation of those effects in the present code would enhance its capabilities. A possible way to achieve this would be by reducing the three-dimensional problem to a set of two-dimensional problems by means of a Galerkin-type decomposition. The presence of a shroud in turbomachinery rows makes this method more appealing than in the case of isolated airfoils.

Acknowledgment

The author is indebted to Professor Paul R. Garabedian of the Courant Institute of Mathematical Sciences for proposing this problem, and for many suggestions and discussions during the development of the code.

References

[1] Bauer, F., Garabedian, P., and Korn, D., *Supercritical Wing Sections*, Vols. I-III, Springer-Verlag, New York, 1972, 1975, and 1977.

[2] Garabedian, P. and Korn, D., "A Systematic Method for Computer Design of Supercritical Airfoils in Cascades," *Communications on Pure and Applied Mathematics*, Vol. XXIX, 1976.

[3] Korn, D., "Numerical Design of Transonic Cascades," *Journal of Computational Physics*, Vol. 29, 1978, pp. 20-34.

[4] Sanz, J., "A Well Posed Boundary Value Problem in Transonic Gas Dynamics," *Communications on Pure and Applied Mathematics*, Vol. XXXI, 1978.

[5] Swenson, E., "Geometry of the Complex Characteristics in Transonic Flows," *Communications on Pure and Applied Mathematics*, Vol. XXI, 1968.

[6] Garabedian, P., *Partial Differential Equations*, Wiley, New York, 1962.